P^{KLM} expansion of the scattering kernel of the nonlinear Boltzmann equation and its convergence rate

G. Kügerl and F. Schürrer
Institute for Theoretical Physics, Technical University of Graz, Petersgasse 16, A-8010 Graz, Austria
(Received 28 July 1988)

A triple expansion of the scattering kernel in terms of Legendre polynomials is used to transform the nonlinear Boltzmann equation into a system of moment equations. The expansion is based on a vector representation of the scattering kernel in the laboratory system, which can be applied to arbitrary collision laws. Low-order approximations result in a remarkable simplification of the moment equations. The rate of convergence of the scattering-kernel expansion is investigated for isotropic scattering in the center-of-mass system. A comparison between the differential scattering and deflecting rate and its approximations define useful truncation indices for practical application.

I. INTRODUCTION

Investigations of Krupp,[1] Krook and Wu,[2] and Bobylev[3] enormously stimulated the application of the nonlinear Boltzmann equation. They discovered independently exact solutions of the nonlinear Boltzmann equation under special conditions, nowadays called the Bobylev-Krook-Wu solution.[4,5] For a simple, but physically interesting initial-value problem they investigated the temporal relaxation to equilibrium of an infinite spatially uniform gas with isotropic initial distributions. The solution of this problem allowed a detailed insight into the approach to equilibrium, even in the spectral range of very high particle energies. This is important in determining chemical reaction rates in the gas phase as well as in plasma physics. The elegance of the exact solution is the result of the restriction that colliding particles interact like Maxwellian molecules, where the scattering cross section is inversely proportional to the relative speed.

For practical applications approximate methods must be developed to solve the nonlinear Boltzmann equation. For this purpose moment methods have gained importance. They are based on an expansion of the particle distribution function in terms of orthogonal polynomials to transform the transport equation into a system of moment equations for easier solution. In the case of simple geometry and simple collision models (e.g., the already mentioned case of relaxation to equilibrium of an isotropic Maxwellian gas) all moments can be evaluated analytically, which consequently results in a complete solution of the transport problem. For general problems the practical advantage of the moment method is based on a series truncation. Grad[6] published one of the first papers on this subject. He used Hermite polynomials as basic functions of his expansions in terms of the particle velocity. Beyond that, Laguerre series were applied.[4,7] Weinert and co-workers[8–11] introduced a generalized moment method, in which the particle distribution was expanded in terms of Burnett basis functions.

The success of the P_N method[12] in neutron transport theory encouraged extension to the nonlinear case.[13] This generalization was based on a vector representation of the scattering kernel. By introducing three variables which define the angles of the collision trihedral, a triple expansion in Legendre polynomials of the differential scattering probability became possible. An additional expansion of the particle distribution function in spherical harmonics enabled us to transform the nonlinear Boltzmann equation into a set of moment equations. It is an advantage of this method that it is applicable to arbitrary collision laws and initial conditions. Beyond that, because of the separation of the speed and direction variables of the particle velocities, this method is also an ideal base for the transformation of the nonlinear Boltzmann equation into a system of multigroup equations. In practice, the choice of low truncation indices results in a remarkable simplification of the moment equations, but the

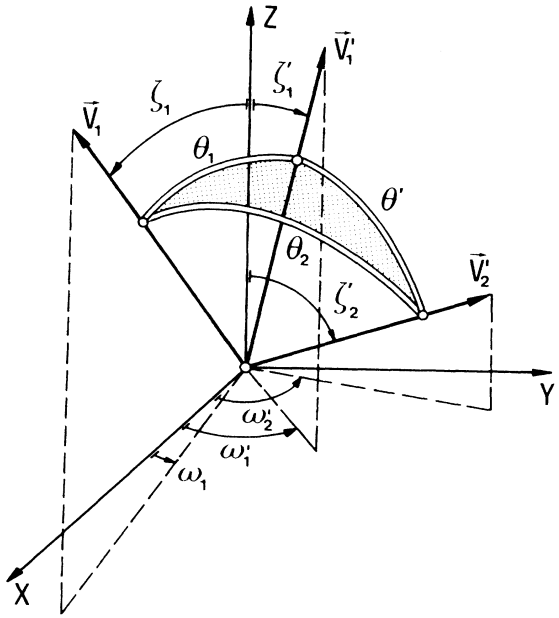

FIG. 1. Collision trihedral in the laboratory system. $\mathbf{v}_1'$ and $\mathbf{v}_1$ are the velocities of the test particle before and after the collision, and $\mathbf{v}_2'$ denotes the initial velocity of the target particle. θ_1 and θ_2 are the first and the second scattering angle, and θ' is the collision angle.

 ©1989 The American Physical Society

quality of this procedure is based on the assumption of a fast convergence of the scattering-kernel expansion, which should be proved in this paper.

In the case of elastic scattering, the differential scattering probability is a singular distribution. Hence, to demonstrate the convergence of its series expansion, we have to use reduced scattering probabilities. To study the dependence on the scattering angle, we introduce the differential deflecting probability. The comparison between the exact representation and different approximations will then define truncation indices apt for practical application. This procedure involves only interactions under a constant collision angle. Therefore the collision-angle distribution is extremely anisotropic. Frequently, the systems under consideration are approximately isotropic and their velocity distribution is of the Maxwellian kind. For this case, it is useful to define differential scattering rates as a function of the temperature and the ratio of the particle speed before and after collision. A comparison with its series expansion proves that it is sufficient to restrict the differential scattering-kernel expansion to a few terms in order to achieve a good approximation. Finally, it is an important result of these investigations that, if we assume an isotropic velocity distribution, only diagonal elements of the triple expansion of the scattering kernel contribute to the scattering rate. This simplifies the moment equations in the cases of isotropic or approximately isotropic velocity distributions substantially.

II. P_N^{KLM} METHOD

The nonlinear Boltzmann equation

$$\frac{\partial}{\partial t}f(\mathbf{r},\mathbf{v}_1,t)+\mathbf{v}_1\nabla_r f(\mathbf{r},\mathbf{v}_1,t)+f(\mathbf{r},\mathbf{v}_1,t)\int d\mathbf{v}_2 f(\mathbf{r},\mathbf{v}_2,t)|\mathbf{v}_1-\mathbf{v}_2|\sigma(|\mathbf{v}_1-\mathbf{v}_2|)$$
$$=\int\int d\mathbf{v}_1' d\mathbf{v}_2' f(\mathbf{r},\mathbf{v}_1',t)f(\mathbf{r},\mathbf{v}_2',t)|\mathbf{v}_1'-\mathbf{v}_2'|\sigma(|\mathbf{v}_1'-\mathbf{v}_2'|)w(\mathbf{v}_1'\rightarrow\mathbf{v}_1;\mathbf{v}_2')+Q(\mathbf{r},\mathbf{v}_1,t) \quad (1)$$

governs the particle distribution density $f(\mathbf{r},\mathbf{v}_1,t)$ within a one-component system. $Q(\mathbf{r},\mathbf{v}_1,t)$ denotes the source density. The product of the relative speed of the colliding particles $|\mathbf{v}_1'-\mathbf{v}_2'|$ (the primed velocities are the anticollisional ones), the integral scattering cross section $\sigma(|\mathbf{v}_1'-\mathbf{v}_2'|)$, and the differential scattering probability define the scattering kernel

$$S=|\mathbf{v}_1'-\mathbf{v}_2'|\sigma(|\mathbf{v}_1'-\mathbf{v}_2'|)w(\mathbf{v}_1'\rightarrow\mathbf{v}_1;\mathbf{v}_2') \; . \quad (2)$$

$w(\mathbf{v}_1'\rightarrow\mathbf{v}_1;\mathbf{v}_2')d\mathbf{v}_1$ is the conditional probability that if the test particle is scattered from $\mathbf{v}_1'$ to between $\mathbf{v}_1$ and $d\mathbf{v}_1$, then the target particle is scattered from $\mathbf{v}_2'$ to any velocity-space element. The trihedral, consisting of the velocities $\mathbf{v}_1'$, $\mathbf{v}_2'$, and $\mathbf{v}_1$, determines this collision process (Fig. 1). It is useful to introduce the angles

$$\begin{aligned}\theta_1&=\arccos[\cos\zeta_1\cos\zeta_1'+\sin\zeta_1\sin\zeta_1'\cos(\omega_1-\omega_1')] \; ,\\ \theta_2&=\arccos[\cos\zeta_1\cos\zeta_2'+\sin\zeta_1\sin\zeta_2'\cos(\omega_1-\omega_2')] \; ,\\ \theta'&=\arccos[\cos\zeta_1'\cos\zeta_2'+\sin\zeta_1'\sin\zeta_2'\cos(\omega_1'-\omega_2')] \; ,\end{aligned} \quad (3)$$

which have the following physical meaning. Test and target particle collide with each other under the "collision angle" θ'. The "first scattering angle" θ_1 is the angle between the incoming and outgoing flight directions of the test particle. The "second scattering angle" θ_2 denotes the angle between the outgoing flight direction of the test particle and the incoming flight direction of the target particle. According to the trihedral consisting of the vectors $\mathbf{v}_1'$, $\mathbf{v}_2'$, and $\mathbf{v}_1$, the angles θ_1, θ_2, and θ' may be interpreted as the sides of a spherical triangle. Therefore the relation

$$\cos(\theta_2+\theta')\leq\cos\theta_1\leq\cos(\theta_2-\theta') \quad (4)$$

determines the domain where the differential scattering probability is defined due to these variables.

In order to apply the spherical harmonics method on the nonlinear Boltzmann equation, we expand the scattering kernel (2) in terms of Legendre polynomials with $\cos\theta_1$, $\cos\theta_2$, and $\cos\theta'$ as arguments:

$$S(v_1,v_1',v_2',\cos\theta_1,\cos\theta_2,\cos\theta')=\sum_{k=0}^{\infty}\sum_{l=0}^{\infty}\sum_{m=0}^{\infty}\frac{(2k+1)(2l+1)(2m+1)}{(4\pi)^3}$$
$$\times S_{klm}(v_1,v_1',v_2')P_k(\cos\theta_1)P_l(\cos\theta_2)P_m(\cos\theta') \; . \quad (5)$$

The scattering-kernel expansion (5) can be applied to arbitrary collision laws. If we assume the scattering to be elastic and isotropic in the center-of-mass system, then the differential scattering probability takes the form

$$w^{\text{c.m.}}(\mathbf{v}_{1_{\text{c.m.}}}'\rightarrow\mathbf{v}_{1_{\text{c.m.}}};\mathbf{v}_{\text{c.m.}}')d\mathbf{v}_{1_{\text{c.m.}}}=\frac{1}{4\pi}\delta(v_{1_{\text{c.m.}}}-v_{1_{\text{c.m.}}}')dv_{1_{\text{c.m.}}}d(\cos\zeta_{1_{\text{c.m.}}})d\omega_{1_{\text{c.m.}}} \; , \quad (6)$$

where we have chosen spherical polar coordinates in the center-of-mass system. The center-of-mass velocity is invariant in the collision process. According to the conservation laws for momentum and energy the particle speed $v_{1_{\text{c.m.}}}'$ is

also conserved, and therefore the differential scattering probability vanishes if $v_{1_{\text{c.m.}}} \neq v'_{1_{\text{c.m.}}}$.

Using Eqs. (3), the transformation of the differential scattering probability (6) into the laboratory system results in[13]

$$w(\mathbf{v}'_1 \rightarrow \mathbf{v}_1;\mathbf{v}'_2)d\mathbf{v}_1 = \frac{1}{\pi}\frac{v_1^2}{v_1'^2+v_2'^2-2v'_1v'_2\cos\theta'}\delta\{[v_1^2+\tfrac{1}{4}(v_1'^2+v_2'^2)+\tfrac{1}{2}v'_1v'_2\cos\theta'-v_1v'_1\cos\theta_1 - v_1v'_2\cos\theta_2]^{1/2}-\tfrac{1}{2}(v_1'^2+v_2'^2-2v'_1v'_2\cos\theta')^{1/2}\} \times dv_1 d(\cos\zeta_1)d\omega_1 \ . \tag{7}$$

The moments of the expansion (5) for isotropic scattering in the center-of-mass system are given by the following integral representation:

$$S_{klm} = 8\pi^2\frac{v_1}{v'_1}\int_{-1}^{1} d(\cos\theta')P_m(\cos\theta')\sigma[(v_1'^2+v_2'^2-2v'_1v'_2\cos\theta')^{1/2}] \times \int_{-1}^{1} d(\cos\theta_2)P_l(\cos\theta_2)P_k\left[\frac{v_1}{v'_1}+\frac{v'_2}{v_1}\cos\theta'-\frac{v'_2}{v'_1}\cos\theta_2\right] \times\Theta\left[\cos(\theta_2-\theta')-\left[\frac{v_1}{v'_1}+\frac{v'_2}{v_1}\cos\theta'-\frac{v'_2}{v'_1}\cos\theta_2\right]\right] \times\Theta\left[\left[\frac{v_1}{v'_1}+\frac{v'_2}{v_1}\cos\theta'-\frac{v'_2}{v'_1}\cos\theta_2\right]-\cos(\theta_2+\theta')\right] . \tag{8}$$

The Θ terms are Heaviside's step functions. On account of Eqs. (3) it is possible to expand the Legendre polynomials in Eq. (5) by means of the addition theorem of Legendre polynomials[14] in terms of the direction variables of the particle velocities in the laboratory system:

$$S = \sum_{k=0}^{\infty}\sum_{l=0}^{\infty}\sum_{m=0}^{\infty}\frac{(2k+1)(2l+1)(2m+1)}{(4\pi)^3}S_{klm} \times\left[P_k(\nu_1)P_k(\nu'_1)+2\sum_{\alpha=1}^{k}\frac{(k-\alpha)!}{(k+\alpha)!}P_k^{\alpha}(\nu_1)P_k^{\alpha}(\nu'_1)\cos[\alpha(\omega_1-\omega'_1)]\right] \times\left[P_l(\nu_1)P_l(\nu'_2)+2\sum_{\beta=1}^{l}\frac{(l-\beta)!}{(l+\beta)!}P_l^{\beta}(\nu_1)P_l^{\beta}(\nu'_2)\cos[\beta(\omega_1-\omega'_2)]\right] \times\left[P_m(\nu'_1)P_m(\nu'_2)+2\sum_{\gamma=1}^{m}\frac{(m-\gamma)!}{(m+\gamma)!}P_m^{\gamma}(\nu'_1)P_m^{\gamma}(\nu'_2)\cos[\gamma(\omega'_1-\omega'_2)]\right] . \tag{9}$$

P_k^{α}, P_l^{β}, and P_m^{γ} symbolize associated Legendre polynomials. Further, we use the abbreviations $\nu_1=\cos\zeta_1$, $\nu_{1'}=\cos\zeta'_1$, and $\nu'_2=\cos\zeta'_2$.

The expansion of the outscattering kernel of Eq. (1) yields

$$|\mathbf{v}_1-\mathbf{v}_2|\sigma(|\mathbf{v}_1-\mathbf{v}_2|)=\sum_{n=0}^{\infty}\frac{2n+1}{4\pi}\sigma_n(v_1,v_2)P_n(\cos\theta) , \tag{10}$$

with

$$\sigma_n(v_1,v_2)=2\pi\int_{-1}^{1}(v_1^2+v_2^2-2v_1v_2\cos\theta)^{1/2}\sigma[(v_1^2+v_2^2-2v_1v_2\cos\theta)^{1/2}]P_n(\cos\theta)d(\cos\theta) , \tag{11}$$

and then, by applying the addition theorem of Legendre polynomials, we obtain the series representation:

$$|\mathbf{v}_1-\mathbf{v}_2|\sigma(|\mathbf{v}_1-\mathbf{v}_2|)=\sum_{n=0}^{\infty}\frac{2n+1}{4\pi}\sigma_n(v_1,v_2)\left[P_n(\nu_1)P_n(\nu_2)+2\sum_{\rho=1}^{n}\frac{(n-\rho)!}{(n+\rho)!}P_n^{\rho}(\nu_1)P_n^{\rho}(\nu_2)\cos[\rho(\omega_1-\omega_2)]\right] . \tag{12}$$

Finally, we expand the particle distribution function and the source density in order to obtain the moment equations. In the case of one-dimensional plane geometry in local space these expansions are given by

$$f(z,v_1,\nu_1,t)=\sum_{n=0}^{\infty}\frac{2n+1}{4\pi}f_n(z,v_1,t)P_n(\nu_1) , \tag{13}$$

with

$$f_n(z,v_1,t)=2\pi\int_{-1}^{1}d\nu_1P_n(\nu_1)f(z,v_1,\nu_1,t) \tag{14}$$

and

$$Q(z,v_1,\nu_1,t)=\sum_{n=0}^{\infty}\frac{2n+1}{4\pi}Q_n(z,v_1,t)P_n(\nu_1)\ , \tag{15}$$

where

$$Q_n(z,v_1,t)=2\pi\int_{-1}^{1}d\nu_1 P_n(\nu_1)Q(z,v_1,\nu_1,t)\ , \tag{16}$$

if we assume an azimuthal symmetrical velocity distribution. Now we insert the series expansions (9), (12), (13), and (15) into Eq. (1), multiply it by $P_i(\nu_1)$, and integrate the resulting equation with respect to ν_1. Taking into account the orthogonality and the recursivity of the Legendre polynomials we obtain the following coupled system of nonlinear moment equations:

$$\begin{aligned}
&\frac{1}{2\pi}\frac{\partial f_n(z,v_1,t)}{\partial t}+\frac{1}{2\pi}\frac{n}{2n+1}v_1\frac{\partial f_{n-1}}{\partial z}+\frac{1}{2\pi}\frac{n+1}{2n+1}v_1\frac{\partial f_{n+1}}{\partial z}\\
&\quad+\sum_{i=0}^{\infty}\sum_{j=0}^{\infty}\frac{(2i+1)(2j+1)}{(4\pi)^2}\alpha_{nij}f_i(z,v_1,t)\int_0^{\infty}dv_2\sigma_j(v_1,v_2)f_j(z,v_2,t)\\
&\quad=\sum_{k=0}^{\infty}\sum_{l=0}^{\infty}\sum_{m=0}^{\infty}\sum_{i=0}^{\infty}\sum_{j=0}^{\infty}\frac{(2k+1)(2l+1)(2m+1)(2i+1)(2j+1)}{(4\pi)^3}\\
&\qquad\times\left[\tfrac{1}{4}\alpha_{kln}\alpha_{kmi}\alpha_{lmj}+\tfrac{1}{2}\sum_{\alpha=1}^{\min(k,l,m)}\frac{(k-\alpha)!(l-\alpha)!(m-\alpha)!}{(k+\alpha)!(l+\alpha)!(m+\alpha)!}\beta_{kln}^{\alpha\alpha}\beta_{kmi}^{\alpha\alpha}\beta_{lmj}^{\alpha\alpha}\right]\\
&\qquad\times\int_0^{\infty}\int_0^{\infty}dv_1'dv_2'S_{klm}(v_1,v_1',v_2')f_i(z,v_1',t)f_j(z,v_2',t)+\frac{1}{2\pi}Q_n(z,v_1,t)\ ,\\
&\qquad\qquad n=0,1,2,3,\ldots
\end{aligned}\tag{17}$$

with

$$f_{-1}(z,v_1,t)=0$$

and

$$\alpha_{ijk}=\int_{-1}^{1}d\nu_1 P_i(\nu_1)P_j(\nu_1)P_k(\nu_1)\ , \tag{18}$$

$$\beta_{ijk}^{\alpha\alpha}=\int_{-1}^{1}d\nu_1 P_i^{\alpha}(\nu_1)P_j^{\alpha}(\nu_1)P_k(\nu_1)\ . \tag{19}$$

The expansion is based on a complete set of functions and therefore the moment equations (17) are equivalent to the original transport equation (1). The practical applicability of this procedure is found by an approximation in truncating the series. In contrast to the P_N method, the truncation index may be chosen differently for the particle density and the scattering kernel. Therefore we name our procedure a P_N^{KLM} method, in analogy to the notation which is generally used in linear transport theory. The choice of low truncation indices results in a remarkable simplification of the moment equations. But it is based on the assumption of a fast convergence of the scattering-kernel expansion. In Secs. III–VI this convergence behavior is particularly investigated.

III. DIFFERENTIAL DEFLECTING PROBABILITY

The differential scattering probability (7) is a singular distribution. For investigating the convergence of its Legendre polynomial expansion, we introduce so-called reduced or integrated scattering probabilities as, for instance,

$$w_{\theta_1}(v_1',v_2',\theta';\theta_1)d(\cos\theta_1)\ ,$$

the differential deflecting probability. This is the probability that if two particles with the initial velocities v_1' (test particle) and v_2' (target particle) collide under the angle θ', then the test particle is scattered to between $\cos\theta_1$ and $\cos\theta_1+d(\cos\theta_1)$.

In order to evaluate the differential deflecting probability we first transform the phase-space element from

$$dv_1 d(\cos\zeta_1)d\omega_1$$

to

$$dv_1 d(\cos\theta_1)d(\cos\theta_2)\ .$$

For that purpose we rotate the coordinate system of Fig. 1, so that the z axis coincides with the direction of $\mathbf{v}_1$, and $\mathbf{v}_2'$ is in the xz plane. To make the transformation one-to-one we restrict the permissible range of ω_1 to the interval $[0,\pi]$. The probability of a particle being scattered into a differential speed solid-angle element cannot depend on the choice of coordinate systems; hence

$$\begin{aligned}
&2w(\mathbf{v}_1'\rightarrow\mathbf{v}_1;\mathbf{v}_2')dv_1 d(\cos\zeta_1)d\omega_1\\
&\quad=\hat{w}(v_1',v_2',\theta';v_1,\theta_1,\theta_2)dv_1 d(\cos\theta_1)d(\cos\theta_2)\ .
\end{aligned}\tag{20}$$

The factor 2 is a result of the restriction of the ω_1 interval to $[0,\pi]$. For every event specified by

$$(v_1,\cos\zeta_1,\omega_1)$$

there is a corresponding one denoted by

$$(v_1,\cos\zeta_1,2\pi-\omega_1) ,$$

which will yield the same value for the differential scattering probability. In the new coordinate system we have, according to Eqs. (3),

$$\begin{aligned}\cos\theta_1&=\cos\zeta_1 ,\\ \cos\theta_2&=\cos\theta_1\cos\theta'+\sin\theta_1\sin\theta'\cos\omega_1 ,\end{aligned} \tag{21}$$

and therefore the Jacobian takes the form

$$\left|\frac{\partial(v_1,\cos\zeta_1,\omega_1)}{\partial(v_1,\cos\theta_1,\cos\theta_2)}\right|=\frac{1}{\{[\cos(\theta_1-\theta')-\cos\theta_2][\cos\theta_2-\cos(\theta_1+\theta')]\}^{1/2}} . \tag{22}$$

It will be suitable to transform the δ function which occurs in Eq. (7) as

$$\begin{aligned}&\delta\{[v_1^2+\tfrac{1}{4}(v_1'^2+v_2'^2)+\tfrac{1}{2}v_1'v_2'\cos\theta'-v_1v_1'\cos\theta_1-v_1v_2'\cos\theta_2]^{1/2}-\tfrac{1}{2}(v_1'^2+v_2'^2-2v_1'v_2'\cos\theta')^{1/2}\}\\ &\qquad=\frac{1}{v_1v_2'}(v_1'^2+v_2'^2-2v_1'v_2'\cos\theta')^{1/2}\delta\left[\cos\theta_2-\left[\frac{v_1}{v_2'}+\frac{v_1'}{v_1}\cos\theta'-\frac{v_1'}{v_2'}\cos\theta_1\right]\right] .\end{aligned} \tag{23}$$

Combining Eqs. (20), (7), (22), and (23), and solving for $\hat{w}$ yields

$$\begin{aligned}\hat{w}(v_1',v_2',\theta';v_1,\theta_1,\theta_2)d\mathbf{v}_1=&\frac{2}{\pi}\frac{v_1}{v_2'}\frac{1}{(v_1'^2+v_2'^2-2v_1'v_2'\cos\theta')^{1/2}}\delta(\cos\theta_2-h_2)\\ &\times\frac{\Theta(\cos(\theta_1-\theta')-\cos\theta_2)\Theta(\cos\theta_2-\cos(\theta_1+\theta'))}{\{[\cos(\theta_1-\theta')-\cos\theta_2][\cos\theta_2-\cos(\theta_1+\theta')]\}^{1/2}}dv_1d(\cos\theta_1)d(\cos\theta_2) ,\end{aligned} \tag{24}$$

with

$$h_2(v_1,v_1',v_2',\theta_1,\theta')=\frac{v_1}{v_2'}+\frac{v_1'}{v_1}\cos\theta'-\frac{v_1'}{v_2'}\cos\theta_1 . \tag{25}$$

The inequalities (4) restrict the domain where $\hat{w}$ is defined with respect to θ_1, θ_2, and θ'. This domain is formally extended to a cube of the side length π by means of Heaviside's step functions.

The following integral defines the differential deflecting probability w_{θ_1}:

$$w_{\theta_1}(v_1',v_2',\theta';\theta_1)d(\cos\theta_1)=\int_0^\infty dv_1\int_{-1}^{1}d(\cos\theta_2)\hat{w}(v_1',v_2',\theta';v_1,\theta_1,\theta_2)d(\cos\theta_1) . \tag{26}$$

If we insert Eq. (24) for $\hat{w}$ and perform the integration over $\cos\theta_1$ we obtain

$$\begin{aligned}w_{\theta_1}(v_1',v_2',\theta';\theta_1)d(\cos\theta_1)=&\frac{2}{\pi}\frac{1}{v_2'}\frac{1}{(v_1'^2+v_2'^2-2v_1'v_2'\cos\theta')^{1/2}}\\ &\times\int_0^\infty dv_1v_1\frac{\Theta(\cos(\theta_1-\theta')-h_2)\Theta(h_2-\cos(\theta_1+\theta'))}{\{[\cos(\theta_1-\theta')-h_2][h_2-\cos(\theta_1+\theta')]\}^{1/2}}d(\cos\theta_1) .\end{aligned} \tag{27}$$

The arguments of the step functions appear as a product in the radical term and lead to special singularities of the integrand. Therefore the numerical integration is done by applying the Gaussian quadrature formula. The solid curves in Figs. 3–5 show numerical results for the exact differential deflecting probability for different collision parameters v_1', v_2', and $\cos\theta'$. We want to emphasize two important properties.

(i) For certain combinations of the collision and scattering angles, the differential deflecting probability vanishes because of the conservation laws for momentum and energy.

(ii) Several parameter combinations result in singularities of w_{θ_1}. Detailed investigations proved that the singular behavior of w_{θ_1} depends on the kind of poles of the integrand. If multiple roots occur in the radicand of Eq. (27) the integral becomes divergent.

We can also construct the differential deflecting probability by means of a vector diagram as shown in Fig. 2. There we consider a collision of two particles specified by the initial velocities $\mathbf{v}_1'$ and $\mathbf{v}_2'$, and collision angle θ'. If we assume isotropic scattering in the center-of-mass system, the points of the possible final velocity vector $\mathbf{v}_{1_{\text{c.m.}}}$ in the center-of-mass system are uniformly distributed on the sphere of radius $v_{1_{\text{c.m.}}}'=v_{1_{\text{c.m.}}}$. This scattering, of course, is not isotropic in the laboratory system. The probability w_{θ_1} that a particle is scattered to between $\cos\theta_1$ and $\cos\theta_1+\Delta(\cos\theta_1)$ will be obtained by means of the following construction. The hatched segment of the unit sphere corresponds to the given scattering angle in-

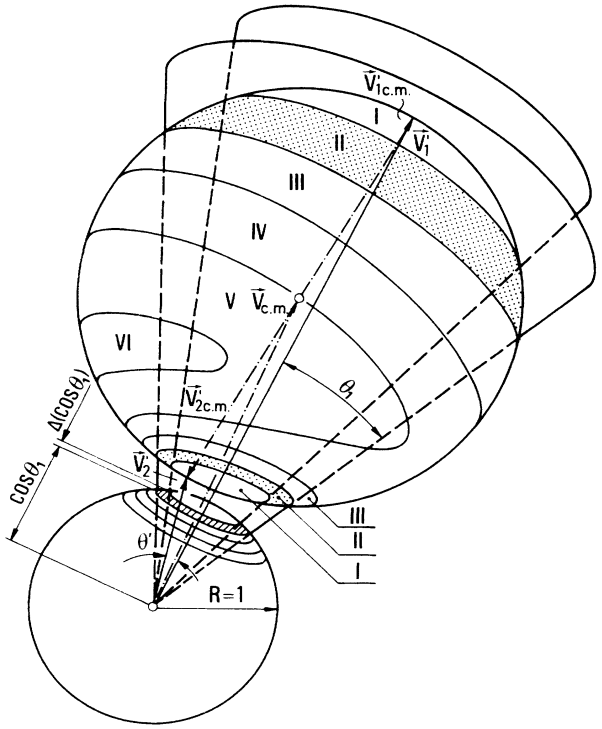

FIG. 2. Geometrical construction of the differential deflecting probability.

terval. The center of the unit sphere and the hatched segment determine two cones whose apex angles are the limits of the given $\cos\theta_1$ interval. The dotted areas in Fig. 2 are defined by the intersection curves of the two cones with the large sphere. The ratio of the dotted area and the sphere is equal to the probability for the deflection into the interval

$$[\cos\theta_1, \cos\theta_1 + \Delta(\cos\theta_1)] .$$

The deflection probability represented in Fig. 5(c) is based on about the same parameter couple v_1'/v_2' and $\cos\theta'$ as the construction in Fig. 2. It is now possible to compare the two results. For $\cos\theta_1 = 1$ the reference area consists of two opposite spherical segments (I). At first, the reference areas (I,II,III) decrease with increasing scattering angle θ_1. A further increase of the apex angle results in a sliding cut between cone and sphere, and therefore the reference area becomes especially large. This is just the scattering angle for which the differential deflecting probability becomes singular. If the apex angle goes beyond a certain value, no interaction occurs and the differential deflecting probability vanishes.

IV. P^{KLM} APPROXIMATION OF THE DIFFERENTIAL DEFLECTING PROBABILITY

The rate of convergence of the scattering-kernel expansion is now studied by comparing the exact differential deflecting probability of Sec. III, with its P^{KLM} approximations. Combining Eqs. (2) and (5) together with Eqs. (20) and (22) yields the P^{KLM} expansion of the differential scattering probability in the $(v_1, \cos\theta_1, \cos\theta_2)$ representation:

$$\hat{w}(v_1', v_2', \theta'; v_1, \theta_1, \theta_2) dv_1 d(\cos\theta_1) d(\cos\theta_2)$$
$$= \frac{2}{|\mathbf{v}_1' - \mathbf{v}_2'|} \frac{1}{\sigma} \frac{\Theta(\cos(\theta_1 - \theta') - \cos\theta_2)\Theta(\cos\theta_2 - \cos(\theta_1 + \theta'))}{\{[\cos(\theta_1 - \theta') - \cos\theta_2][\cos\theta_2 - \cos(\theta_1 + \theta')]\}^{1/2}}$$
$$\times \sum_{k=0}^{K} \sum_{l=0}^{L} \sum_{m=0}^{M} \frac{(2k+1)(2l+1)(2m+1)}{(4\pi)^3} S_{klm}(v_1, v_1', v_2') P_k(\cos\theta_1) P_l(\cos\theta_2) P_m(\cos\theta') dv_1 d(\cos\theta_1) d(\cos\theta_2) . \quad (28)$$

The moments $S_{klm}(v_1, v_1', v_2')$ are given by Eq. (8). Integrating Eq. (28) over v_1 and $\cos\theta_2$ yields the requested differential deflecting probability in the P^{KLM} approximation:

$$w_{\theta_1}^{KLM}(v_1', v_2', \theta'; \theta_1) d(\cos\theta_1) = \frac{2}{|\mathbf{v}_1' - \mathbf{v}_2'|\sigma} \sum_{k=0}^{K} \sum_{l=0}^{L} \sum_{m=0}^{M} \frac{(2k+1)(2l+1)(2m+1)}{(4\pi)^3} I_{klm}(v_1', v_2') J_l(\theta_1, \theta')$$
$$\times P_k(\cos\theta_1) P_m(\cos\theta') d(\cos\theta_1) , \quad (29)$$

with

$$I_{klm}(v_1', v_2') = \int_0^\infty dv_1 S_{klm}(v_1, v_1', v_2') \quad (30)$$

and

$$J_l(\theta_1, \theta') = \int_{-1}^{1} d(\cos\theta_2) P_l(\cos\theta_2) \frac{\Theta(\cos(\theta_1 - \theta') - \cos\theta_2)\Theta(\cos\theta_2 - \cos(\theta_1 + \theta'))}{\{[\cos(\theta_1 - \theta') - \cos\theta_2][\cos\theta_2 - \cos(\theta_1 + \theta')]\}^{1/2}} . \quad (31)$$

The coefficients I_{klm} are to be calculated numerically, assuming $\sigma = \text{const}$, and the integral in Eq. (31) can be evaluated analytically. Using the subsitution

$$\cos\alpha = \frac{\cos\theta_2 - \cos\theta_1 \cos\theta'}{\sin\theta_1 \sin\theta'} ,$$

Eq. (31) can be written as

$$J_l(\theta_1,\theta')=\int_0^{\pi} d\alpha\, P_l(\cos\theta_1\cos\theta'+\sin\theta_1\sin\theta'\cos\alpha)\ . \tag{32}$$

Now we apply the addition theorem of Legendre polynomials and obtain

$$J_l(\theta_1,\theta')=\int_0^{\pi} d\alpha \left[P_l(\cos\theta_1)P_l(\cos\theta')+2\sum_{m=1}^{l}\frac{(l-m)!}{(l+m)!}P_l^m(\cos\theta_1)P_l^m(\cos\theta')\cos(m\alpha)\right]\ . \tag{33}$$

The integration with respect to α results immediately in

$$J_l(\theta_1,\theta')=\pi P_l(\cos\theta_1)P_l(\cos\theta')\ . \tag{34}$$

Figures 3–5 show the comparison of P^{KLM} approximations of the differential deflecting probability for different velocities and collision angles with exact results. Because of the $\cos\theta_1$ dependence in Eq. (29), the P^{KLM} approximations are curves of $(K+L)$th order. Therefore any approximation due to the index triple $(0,0,M)$ with arbitrary M is a horizontal line. The P^{01M} as well as the P^{10M} approximation are straight lines of positive or negative slope. The plots in Figs. 3(b), 4(b), and 5(b) are to be considered as special cases. According to the assumption $\cos\theta'=0$ only terms of even index l and m make a contribution to the sum in Eq. (29). [$P_i(\cos\theta')$ vanishes if $\cos\theta'=0$ and i is an odd number.] Discontinuities and singularities in Figs. 3(c), 4(c), and 5(c) would require a high-order approximation. But for practical solutions of the moment equations (17), low-order approximations are necessary. The P^{000} approximation provides only a constant value, but its order of magnitude is acceptable as illustrated in Figs. 3(a), 3(b), 4(a), 4(c), and 5(b). The approximation is essentially improved if we choose the truncation triple (1,1,1) [see Figs. 3(a), 4(a), and 4(c)]. Starting from the P^{111} approximation to increase one of the three indices results only in a negligible correction [see Figs. 3(c), 5(a), and 5(c)]. However, if we increase the other indices too, a further improvement can be obtained as shown in Fig. 4(b). In summation, we note that it is possible to approximate the differential scattering probability in a quantitatively satisfactory way using truncation indices $K,L,M\le 3$. But it should be noticed that our research was based on an extremely anisotropic test case—the collision angle θ' was kept constant. Hence the rate of convergence is not as good as in the isotropic case, which will be proved in Secs. V and VI.

V. MAXWELL-AVERAGED DIFFERENTIAL SCATTERING RATE

We consider the Maxwell-averaged differential scattering rate $R(v_1'\to v_1)dv_1$ as a further test case to investigate the convergence of the differential scattering probability expansion. This rate is to be interpreted as the probability that a test particle at initial speed v_1' interacting with target particles of Maxwellian velocity distribution will be scattered to between v_1 and v_1+dv_1. We apply the collison law valid for rigid spheres, $\sigma=\sigma_0=$const. The differential scattering probability $\hat{w}$ is then given by Eq. (24). Assuming the target particles to be Maxwellian distributed, as

$$M(v_2')dv_2'd(\cos\theta')=2\pi(\pi v_w^2)^{-3/2}v_2'^2 \times\exp\left[-\left[\frac{v_2'}{v_w}\right]^2\right]dv_2'd(\cos\theta')\ , \tag{35}$$

makes this example comparable to practical applications. The density of the target gas is normalized to 1 and

$$v_w=\left[\frac{2kT}{m}\right]^{1/2} \tag{36}$$

denotes the most probable speed of target particles. Thus the Maxwell-averaged differential scattering rate is given by

$$R(v_1'\to v_1)dv_1=\int_0^{\infty}dv_2'M(v_2')\int_{-1}^{1}d(\cos\theta')\int_{-1}^{1}d(\cos\theta_1)\int_{-1}^{1}d(\cos\theta_2)|\mathbf{v}_1'-\mathbf{v}_2'|\sigma_0\hat{w}(v_1',v_2',\theta';v_1,\theta_1,\theta_2)dv_1\ . \tag{37}$$

Because of the δ function in $\hat{w}$ [see Eq. (24)], the integration over $\cos\theta_2$ is immediate and Eq. (37) turns into the triple-integral formulation

$$R(v_1'\to v_1)dv_1=\frac{2\sigma_0 v_1}{\pi}\int_0^{\infty}dv_2'\frac{M(v_2')}{v_2'}\int_{-1}^{1}d(\cos\theta')\int_{-1}^{1}d(\cos\theta_1)\frac{\Theta(\cos(\theta_1-\theta')-h_2)\Theta(h_2-\cos(\theta_1+\theta'))}{\{[\cos(\theta_1-\theta')-h_2][h_2-\cos(\theta_1+\theta')]\}^{1/2}}dv_1\ . \tag{38}$$

h_2 is given by Eq. (25). With the abbreviations

$$A=\cos\theta_1\cos\theta'-h_2\ ,\qquad B=\sin\theta_1\sin\theta'\ , \tag{39}$$

the integral over $\cos\theta_1$ in Eq. (38) can be written as

$$\int_{-1}^{1}d(\cos\theta_1)\frac{\Theta(B+A)\Theta(B-A)}{[(B+A)(B-A)]^{1/2}}\ . \tag{40}$$

The product of step functions in Eq. (40) is equivalent to the condition

$$|A|\le B\ , \tag{41}$$

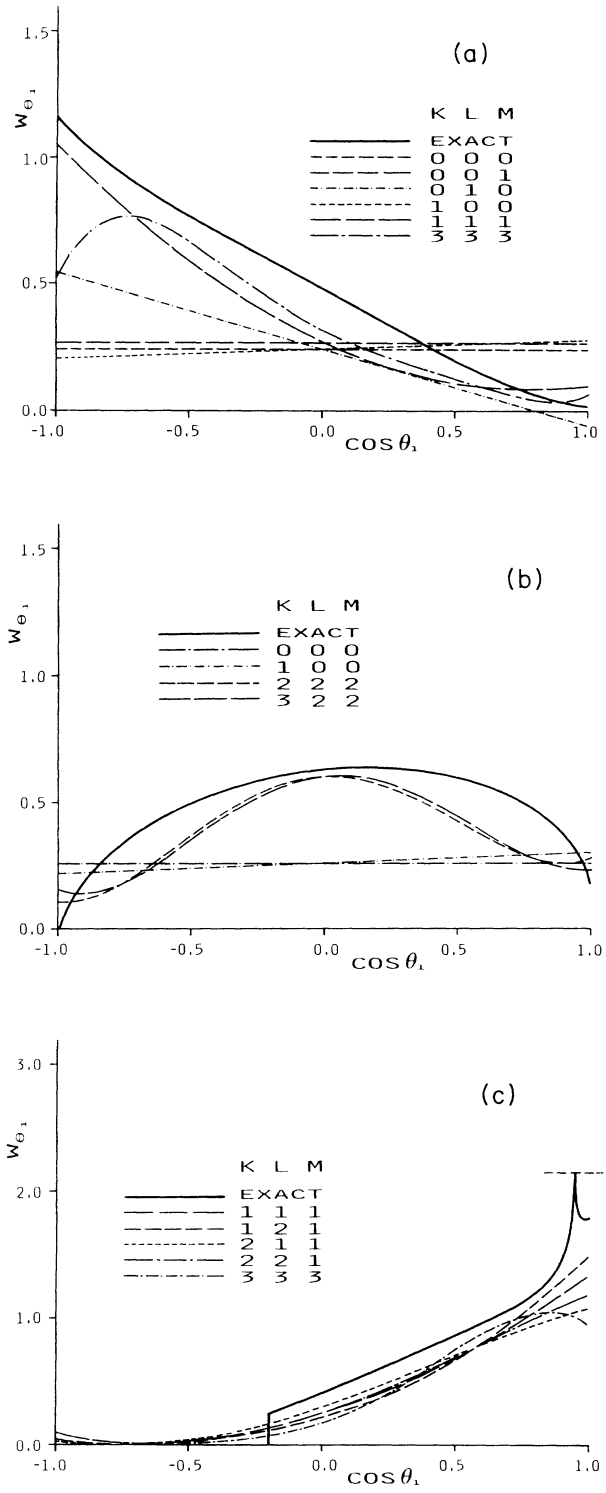

FIG. 3. Comparison of the exact differential deflecting probability w_{θ_1} with various P^{KLM} approximations as a function of the cosine of the first scattering angle θ_1. Ratio of the test and target particle velocity before the collision $v_1'/v_2'=0.1$. Cosine of the collision angle: (a) $\cos\theta'=-0.707$, (b) $\cos\theta'=0$, and (c) $\cos\theta'=0.707$.

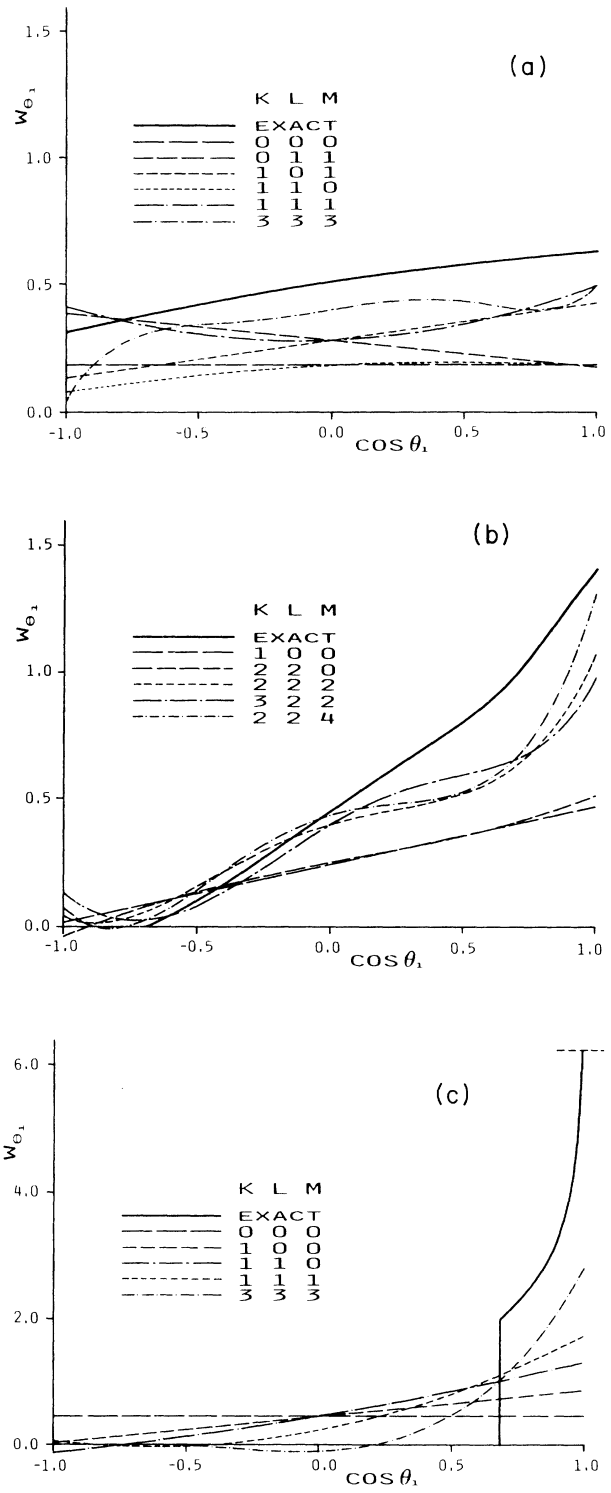

FIG. 4. Comparison of the exact differential deflecting probability w_{θ_1} with various P^{KLM} approximations as a function of the cosine of the first scattering angle θ_1. Ratio of the test and target particle velocity before the collision $v_1'/v_2'=1$. Cosine of the collison angle: (a) $\cos\theta'=-0.707$, (b) $\cos\theta'=0$, and (c) $\cos\theta'=0.707$.

which results in a further limitation of the domain of integration:

$$x_1 \leq \cos\theta_1 \leq x_2 \ , \tag{42}$$

and we find

$$x_{1,2} = \frac{ab \mp [c^2(b^2+c^2-a^2)]^{1/2}}{(b^2+c^2)} \ . \tag{43}$$

For the inequality

$$b^2+c^2-a^2 \leq 0 \tag{44}$$

the integral vanishes too. The terms a, b, and c are given by

$$\begin{aligned} a &= \frac{v_1}{v_2'} + \frac{v_1'}{v_1}\cos\theta' \ , \\ b &= \frac{v_1'}{v_2'} + \cos\theta' \ , \\ c &= \sin\theta' \ . \end{aligned} \tag{45}$$

We then represent the polynomial of the radical term of Eq. (40) as a product of its roots and obtain instead

$$\frac{\Theta(b^2+c^2-a^2)}{(b^2+c^2)^{1/2}} \int_{x_1}^{x_2} d(\cos\theta_1) \frac{1}{[(\cos\theta_1 - x_1)(x_2 - \cos\theta_1)]^{1/2}} \ . \tag{46}$$

This is a special case of integral (31). Hence we obtain for $l=0$ according to Eq. (34):

$$\pi \frac{\Theta(b^2+c^2-a^2)}{(b^2+c^2)^{1/2}} \ , \tag{47}$$

and the Maxwell-averaged differential scattering rate (38) results in

$$R(v_1' \rightarrow v_1)dv_1 = 2\sigma_0 v_1 \int_0^\infty dv_2' \frac{M(v_2')}{v_2'} \int_{-1}^{1} d(\cos\theta') \frac{\Theta\left(1+\left[\frac{v_1'}{v_2'}\right]^2 - \left[\frac{v_1}{v_2'}\right]^2 - \left[\frac{v_1'}{v_1}\right]^2 \cos^2\theta'\right)}{\left[1+\left[\frac{v_1'}{v_2'}\right]^2 + 2\frac{v_1'}{v_2'}\cos\theta'\right]^{1/2}} \ . \tag{48}$$

Integrating over $\cos\theta'$ we get

$$R(v_1' \rightarrow v_1) = 4\sigma_0 \left[\frac{v_1}{v_1'} \int_0^{v_1} dv_2' M(v_2') + \frac{v_1^2}{v_1'} \int_{v_1}^\infty dv_2' \frac{M(v_2')}{v_2'} \right]$$

for downscattering ($v_1 \leq v_1'$), and

$$R(v_1' \rightarrow v_1) = 4\sigma_0 \left[\frac{v_1}{v_1'} \int_{(v_1^2 - v_1'^2)^{1/2}}^{v_1} dv_2' \frac{(v_1'^2 + v_2'^2 - v_1^2)^{1/2}}{v_2'} M(v_2') + v_1 \int_{v_1}^\infty dv_2' \frac{M(v_2')}{v_2'} \right]$$

for upscattering ($v_1 > v_1'$). Finally, using Eq. (35) and integrating over v_2' yields

$$R(v_1' \rightarrow v_1) = \begin{cases} 2\sigma_0 \dfrac{v_1}{v_1'} \operatorname{erf}\left[\dfrac{v_1}{v_w}\right] & v_1 \leq v_1' \\ 2\sigma_0 \dfrac{v_1}{v_1'} \exp\left[-\dfrac{v_1^2 - v_1'^2}{v_w^2}\right] \operatorname{erf}\left[\dfrac{v_1'}{v_w}\right] & v_1 > v_1' \ . \end{cases} \tag{49}$$

This result agrees with that quoted by Williams[15] and Heinrichs[16] for the differential scattering rate and the effective differential scattering cross section, respectively,

$$\sigma_{\text{eff}}(v_1' \rightarrow v_1) = \frac{1}{v_1'} R(v_1' \rightarrow v_1) \ ,$$

but it was found in a quite different manner. A three-dimensional plot of the Maxwell-averaged differential scattering rate (49) is given in Fig. 6.

VI. P^{KLM} APPROXIMATION OF THE MAXWELL-AVERAGED DIFFERENTIAL SCATTERING RATE

Introducing the series expansion (28) of the differential scattering probability into Eq. (37) yields the P^{KLM} approximation of the Maxwell-averaged differential scattering rate as

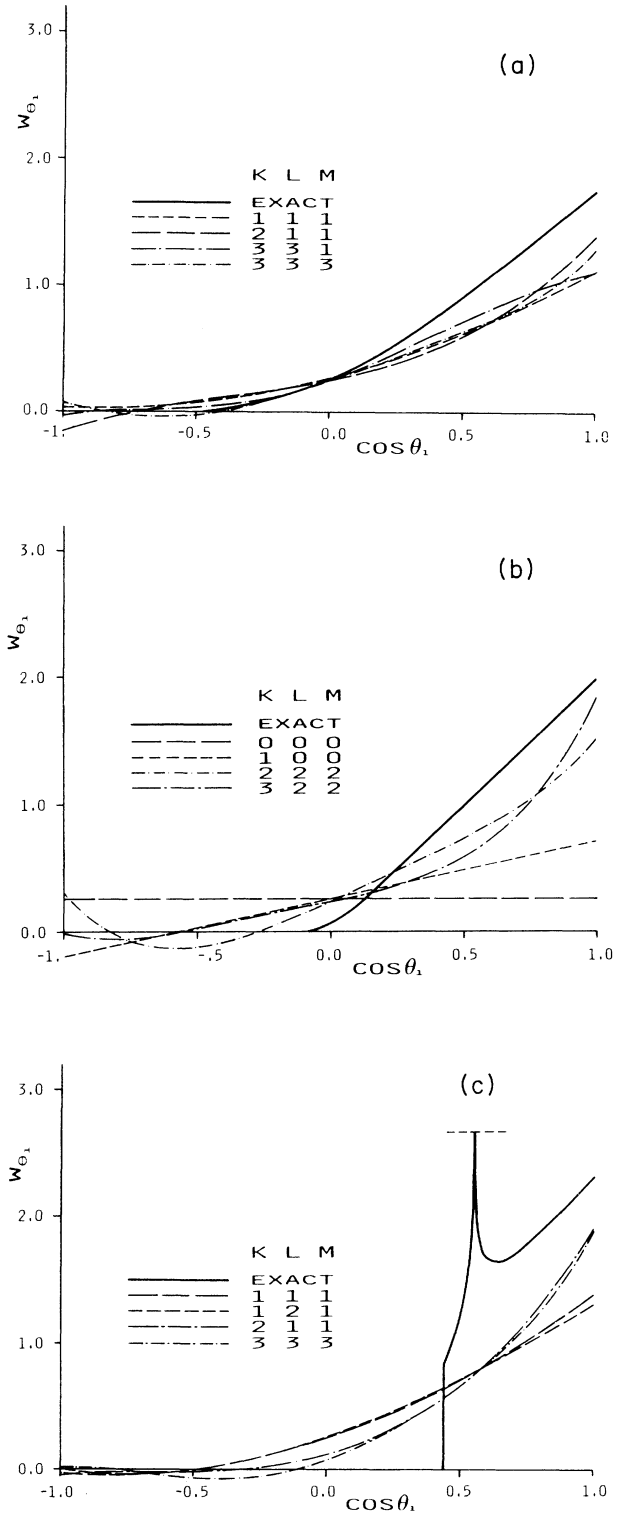

FIG. 5. Comparison of the exact differential deflecting probability w_{θ_1} with various P^{KLM} approximations as a function of the cosine of the first scattering angle θ_1. Ratio of the test and target particle velocity before the collision $v_1'/v_2'=10$. Cosine of the collision angle: (a) $\cos\theta'=-0.707$, (b) $\cos\theta'=0$, and (c) $\cos\theta'=0.707$.

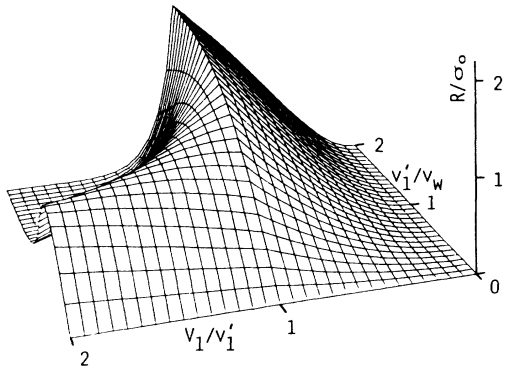

FIG. 6. Maxwell-averaged differential scattering rate $R(v_1'\rightarrow v_1)$ in units of the cross section σ_0 as a function of the inverse ratio of the particle speed before and after the collision v_1' and v_1, and the ratio of the speed of the incoming test particle v_1' and the most probable velocity of the particles of the target gas v_w.

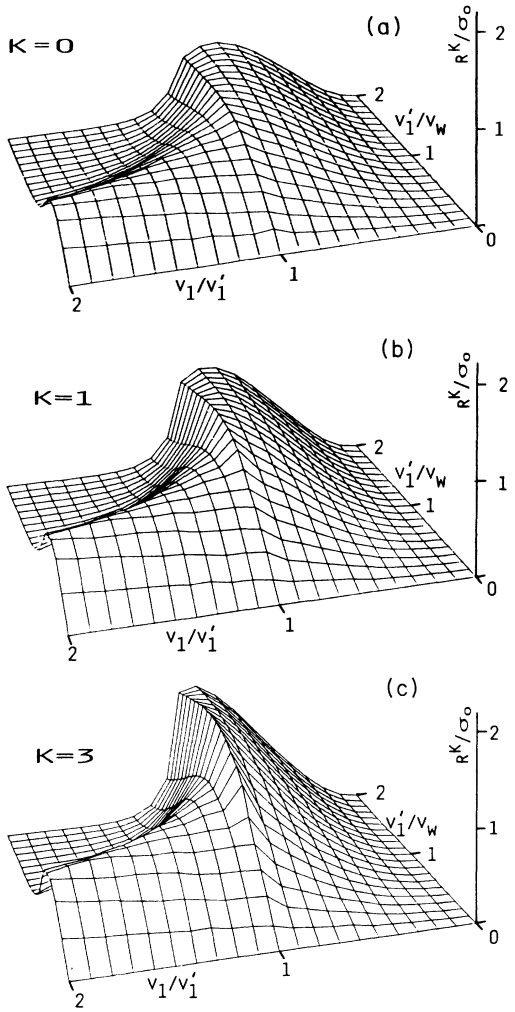

FIG. 7. P^K approximations of the Maxwell-averaged differential scattering rate for various truncation indices; (a) $K=0$, (b) $K=1$, and (c) $K=3$. The scale is the same as in Fig. 6.

$$R^{KLM}(v_1' \to v_1) = \sum_{k=0}^{K} \sum_{l=0}^{L} \sum_{m=0}^{M} \frac{(2k+1)(2l+1)(2m+1)}{(4\pi)^3} \rho_{klm}(v_1, v_1') \pi_{klm} \ , \tag{50}$$

with

$$\rho_{klm}(v_1, v_1') = 2 \int_0^\infty dv_2' M(v_2') S_{klm}(v_1, v_1', v_2') \tag{51}$$

and

$$\pi_{klm} = \int_{-1}^{1} d(\cos\theta') P_m(\cos\theta') \times \int_{-1}^{1} d(\cos\theta_1) P_k(\cos\theta_1) \int_{-1}^{1} d(\cos\theta_2) P_l(\cos\theta_2) \frac{\Theta(\cos(\theta_1 - \theta') - \cos\theta_2)\Theta(\cos\theta_2 - \cos(\theta_1 + \theta'))}{\{[\cos(\theta_1 - \theta') - \cos\theta_2][\cos\theta_2 - \cos(\theta_1 + \theta')]\}^{1/2}} \ . \tag{52}$$

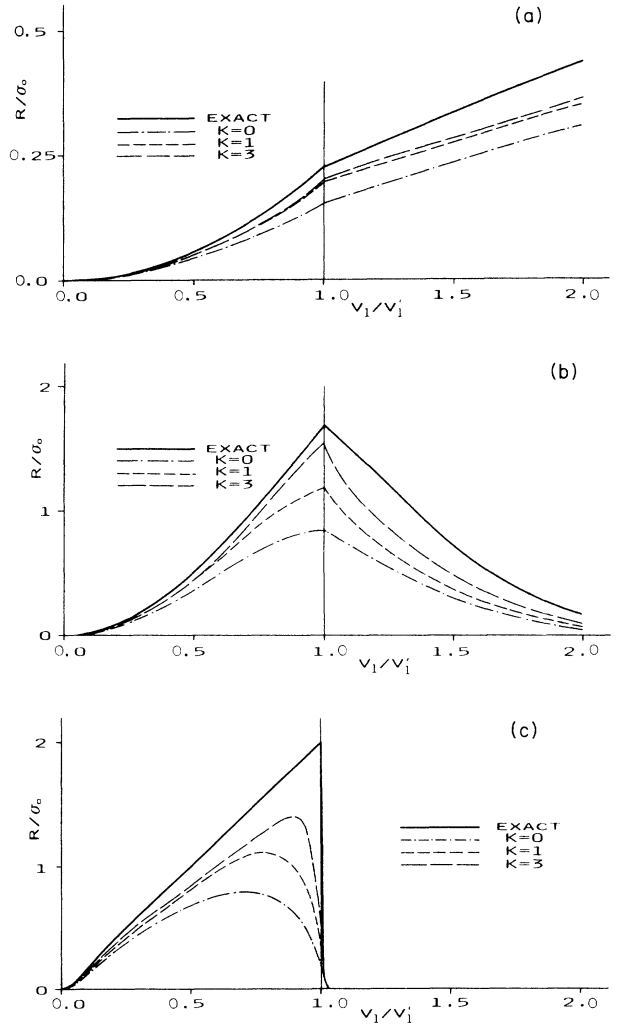

FIG. 8. Maxwell-averaged differential scattering rate $R(v_1' \to v_1)$ and various P^K approximations in units of the cross section σ_0 as a function of the inverse ratio of the particle speed before and after the collision v_1' and v_1. Ratio of the speed of the incoming test particle v_1' and the most probable velocity of the particles of the target gas v_w: (a) $v_1'/v_w = 0.1$, (b) $v_1'/v_w = 1$, and (c) $v_1'/v_w = 10$.

The Maxwell distribution $M(v_2')$ and the moments S_{klm} are given by Eqs. (35) and (8), respectively. The coefficients π_{klm} involve an integral over $\cos\theta_2$ of the type given in Eq. (31). The result of this integration reduces Eq. (52) by means of Eq. (34) to a double-integral expression and finally, by applying the orthogonality relation of Legendre polynomials we obtain

$$\pi_{klm} = \pi \left[\frac{2}{2k+1} \right]^2 \delta_{kl} \delta_{lm} \ . \tag{53}$$

Thus all off-diagonal elements of the triple expansion in Eq. (50) vanish, and we get a result which is similar to a P^K approximation of the Maxwell-averaged differential scattering rate:

$$R^K(v_1' \to v_1) = \sum_{k=0}^{K} \frac{2k+1}{(4\pi)^2} \rho_{kkk}(v_1, v_1') \ . \tag{54}$$

The coefficients ρ_{kkk} are to be calculated numerically. Figures 7(a)–7(c) display in a three-dimensional representation the convergence behavior of the P^K approximation of the Maxwell-averaged differential scattering rate. A comparison of the exact scattering rate with various degrees of approximation, $K = 0$, 1, and 3, is given in Figs. (8)–8(c). From these figures we can see that already a few terms of the expansion result in a good agreement with the exact behavior.

It is remarkable that for isotropic velocity distributions the off-diagonal elements of the P^{KLM} approximation of the differential scattering rate vanish. This behavior allows an important simplification of the moment equations (17). Thus, for isotropic distributions, only terms in conjunction with S_{kkk} contribute to the fivefold sum of the inscattering term in Eqs. (17). If the distributions are approximately isotropic, contributions from off-diagonal terms are negligible, and the fivefold sum reduces to a triple one. We expect that for determining particle distributions of approximately isotropic velocity distributions, the P_N^{KLM} method will become similarly as important as the P_N method in linear transport theory.

[1]R. S. Krupp, M. Sc. thesis, Massachusetts Institute of Technology, Cambridge, MA, 1967.
[2]M. Krook and T. T. Wu, Phys. Fluids **20**, 1589 (1977).
[3]A. V. Bobylev, Dokl. Akad. Nauk SSSR **225**, 1296 (1975) [Sov. Phys.—Dokl. **20**, 822 (1976)].
[4]M. H. Ernst, Phys. Rep. **78**, 1 (1981).
[5]M. H. Ernst, J. Stat. Phys. **34**, 1001 (1984).
[6]H. Grad, in *Principles of the Kinetic Theory of Gases,* Vol. 12 of *Handbuch der Physik,* edited by S. Flügge (Springer-Verlag, Berlin, 1958).
[7]M. H. Ernst, Phys. Lett. **69A**, 390 (1979).
[8]U. Weinert and K. Suchy, Z. Naturforsch. Teil A **32**, 390 (1977).
[9]U. Weinert, Z. Naturforsch. Teil A **33**, 480 (1978).
[10]U. Weinert, J. Math. Phys. **20**, 2339 (1979).
[11]U. Weinert, S. L. Lin, and E. A. Mason, Phys. Rev. A **22**, 2262 (1980).
[12]M. M. R. Williams, *Mathematical Methods in Particle Transport Theory* (Butterworths, London, 1971).
[13]F. Schürrer, Atomkernenergie-Kerntech. **46**, 238 (1985).
[14]W. Magnus, F. Oberhettinger, and R. P. Soni, *Formulas and Theorems for the Special Functions of Mathematical Physics* (Springer-Verlag, Berlin, 1966).
[15]M. M. R. Williams, *The Slowing Down and Thermalization of Neutrons* (North-Holland, Amsterdam, 1966), p. 25.
[16]G. Heinrichs, M. Sc. thesis, Technical University of Graz, 1986).